Forest Science, Vol. 34, No. 2, pp. 259–275.

Classification of Airborne Multispectral Scanner Data for Mapping Current Defoliation Caused by the Spruce Budworm

DONALD G. LECKIE
DONALD P. OSTAFF

ABSTRACT. Airborne multispectral scanner data were acquired over a mixed fir and spruce forest affected by both current defoliation (red discoloration) and cumulative defoliation (loss of needles) caused by feeding of the spruce budworm (*Choristoneura fumiferana* [Clem]). The spectral bands, ratios and differences of bands, and principal components derived from the bands were examined for their usefulness for discriminating defoliation condition. Classifications were conducted using the best combinations of two through nine bands or features derived from the bands. Three levels of current defoliation could be classified (heavy, light, and healthy). Cumulative defoliation and mixed-wood areas caused confusions in the classifications. There was little advantage to including more than four bands or derived features in the classifications. FOR. SCI. 34(2):259–275.

ADDITIONAL KEY WORDS. Damage assessment, cumulative defoliation, feature selection, remote sensing, maximum likelihood classification.

THE SPRUCE BUDWORM *Choristoneura fumiferana* is probably the most important influence in the management of spruce-fir forests in many regions of eastern North America. Repeated annual feeding on current year foliage results in loss of radial or volume increment, reduced or complete loss of height growth, tree mortality, and decreased stand yields. The current spruce budworm outbreak in eastern North America started in the late 1960s in northeastern Ontario, western Quebec, central New Brunswick, and Maine (Kettela 1983). By 1975, the outbreak covered 57 million ha in eastern North America and, by 1983, 23 million ha of susceptible forest contained significant volumes of dead and dying timber. Because outbreaks can seriously disrupt long-term timber supply and subsequent industrial viability, information on the amount and location of budworm damage is necessary for the development of stand management strategies.

Budworm defoliation mapping programs are implemented in most outbreak areas. Each year susceptible forests are sketch-mapped from light aircraft in order to outline the areas of forest defoliated by the budworm during that year (current defoliation). This information is used as part of a hazard rating system, which influences protection programs and stand harvesting schedules (Dorais and Kettela 1982).

The feeding habits of the budworm result in damage symptoms that facili-

Donald Leckie is with the Petawawa National Forestry Institute, Canadian Forestry Service, Chalk River, Ontario, KOJ 1JO, and Donald Ostaff is with the Canadian Forestry Service—Maritimes, P.O. Box 4000, Fredericton, N.B. E3B 5P7. The authors wish to thank Forest Protection Limited of Fredericton, N.B., for providing logistical support, especially light aircraft for acquiring oblique photographs and sketch-map information, Maritime Resource Management Service for providing the colour infrared photographs, and E. G. Kettela of the Canadian Forestry Service—Maritimes for acquiring sketch-map data for the test area. Manuscript received December 24, 1986.

tate the mapping of current defoliation. After overwintering as second instar larvae, the budworm begins feeding in late April–early May on vegetative or pollen buds, old foliage, and on the expanding current year shoots. By early June the budworm reaches the sixth instar, a stage that accounts for 87% of the total amount of food consumed during the budworm's life cycle (Miller 1977). The larvae feed within "tunnels" composed of two or three shoots webbed together. Feeding generally occurs on the needles of the current year shoots but can occur on older foliage, particularly when population levels are high. Partially consumed needles and other feeding debris become caught in these tunnels. When population levels are high, these needles, having turned red, and other feeding debris give the trees a characteristic red color. It is this red coloration that is assessed through aerial sketch-mapping. Mapping of the red coloration of current defoliation gives an approximation of the distribution and level of budworm populations, as well as the amount of damage that has occurred that year. Timing for mapping defoliation is therefore critical because peak coloration occurs during a relatively short period, generally in late June to early July. Wind and rain eventually knock the red needles and other feeding debris from the trees, leaving exposed branches. Successive years of defoliation will result in loss of several age classes of needles and exposure of bare twigs (cumulative defoliation). Mortality may occur.

Aerial sketch-mapping is a simple, quick, and inexpensive method appropriate for acquiring a rough delineation of insect damage but has drawbacks if accurate delineations are required (Harris and Dawson 1979). Attempts have been made to improve the accuracy of defoliation estimates by using aerial photographs. Murtha (1973) used 1:10,000 color infrared photographs to stratify spruce-fir stands damaged by the spruce budworm into five defoliation and mortality classes. Ashley et al (1976) demonstrated that normal color summer aerial photographs at scales of 1:15,840 and larger were appropriate for evaluating current defoliation. Current-year defoliation caused by the western spruce budworm *Choristoneura occidentalis* Freeman could not be detected using ultra small scale (1:126,000) color infrared photographs (Ciesla 1974). Studies have indicated that Landsat multispectral scanner (MSS) data have low capabilities for detecting and delineating current spruce budworm defoliation (Harris et al. 1978, Madding and Hogan 1978). The unreliability of acquiring cloud-free satellite imagery during the short critical period when red discolored foliage is visible on trees limits the usefulness of satellite data. Airborne multispectral scanner data with their higher spatial resolution, greater number of wavelength bands, and flexibility in timing data acquisition may provide a suitable tool for assessing current defoliation.

The purpose of this study was to evaluate the effectiveness of airborne multispectral scanner data for detecting, mapping, and quantifying the red coloration of current defoliation.

METHODS

Test Area

An area in northern New Brunswick (5 × 30 km at latitude 47°20'N and longitude 67°21'W) was selected as a test site (Sisson Reservoir test area). The test area was generally flat or gently sloping. Some areas had broad hills with relief up to 75 m. Hardwoods occurred frequently on the hill crowns. There were occasional steep but short-sided valleys.

The forest consisted of softwood, mixed-wood, and hardwood stands of varying areal extents. Softwood stands were often small in area. The predominant softwood species were balsam fir (*Abies balsamea* [L.] Mill), and spruce, mainly white spruce (*Picea glauca* [Moench] Voss). These generally occurred in mixed stands with compositions of predominantly fir (fir-spruce) to stands of predominantly spruce (spruce-fir). Eastern white cedar (*Thuja occidentalis* L.) and tamarack (*Larix laricina* [DuRoi] K. Koch) occurred along stream courses and in lowland areas. The condition of the mixed fir and spruce stands at the time of data acquisition varied from healthy (no defoliation) to severe current defoliation, with many of the stands also having varying degrees of cumulative defoliation (lack of foliage due to defoliation of previous years), including mortality. Defoliation conditions may not be consistent throughout a stand, and mixtures of different defoliation conditions can occur within stands. Current and cumulative defoliation also occurred on the softwoods within the mixed-wood stands.

DATA ACQUISITION

Eleven channel airborne MSS data were acquired on a single flight line over the Sisson Reservoir test area at 0935 hr Atlantic Daylight Time on July 3, 1981, during the peak period of current defoliation caused by budworm feeding. Solar altitude was 37° and solar azimuth 95°, which was 55° from the flight line azimuth (220°). The data were acquired by the Canada Centre for Remote Sensing using a Daedalus 1260 multispectral scanner mounted in a DC-3 aircraft (Zwick et al. 1980). The scanner had a 37° field of view each side of nadir. Flying altitude was 3650 m above ground level, which, with the 2.5 mr resolution of the scanner, resulted in an image with a spatial resolution of approximately 9-m. This resolution is practical for broad area damage surveys and gives results appropriate for resolutions with at least several trees per pixel and several pixels per homogeneous damage area. The wavelengths of the bands of the scanner are listed in Table 1. Bands 1 and 2 were not used in this study due to low signal-to-noise ratios typical of these bands. The MSS data of each band had radiometric distortions across the image due to atmospheric effects and sun-object-viewer geometry (e.g., viewing sunlit trees on one side of the image and backlit trees on the other side of the image). The distortions in each band were modelled by a least squares polynomial fit of the mean pixel intensity of defoliated stands versus

TABLE 1. Airborne Multispectral Scanner bands.

Band[1]	Wavelength (μm)
1	0.39–0.42
2	0.42–0.45
3	0.45–0.50
4	0.50–0.55
5	0.55–0.60
6	0.59–0.65
7	0.63–0.70
8	0.68–0.78
9	0.77–0.90
10	0.87–1.04
11	1.55–2.75

[1] Bands 1 through 10 are from Zwick et al. (1980) and band 11 from McColl, W.D. (pers. comm.).

the position of the stand from nadir. The distortions were corrected by adding to each band a correction factor derived from the models such that models describing the intensity of defoliated stands across the corrected images have a uniform distribution. Data near the edges of the images (view angles greater than 28°) were not used in the analysis of this study due to possible inaccuracies in the correction at extreme view angles.

Simultaneous 1:24,000 normal color aerial photographs were also obtained. Additional 1:11,000 and 1:4,000 normal color and 1:5,500 color infrared aerial photographs were taken for segments of the test area. Oblique 35 mm photographs were also obtained from a light aircraft at altitudes of 490 m, 180 m, and 90 m above ground level. The additional aerial and oblique photographs were acquired the same day as the airborne MSS data. A detailed defoliation aerial sketch-map of the test area was obtained July 5.

Defoliation Classes and Selection of Sample Training Areas

The defoliation classes used in this study were defined as follows:

healthy—no visible current or cumulative defoliation and no mortality

light defoliation—current defoliatin less than 35%; generally having less than 10–15% cumulative defoliation

moderate defoliation—current defoliation 35–70%; generally having less than 20% cumulative defoliation

severe defoliation—current defoliation >70%; generally having less than 20% cumulative defoliation

moderate cumulative defoliation—cumulative defoliation between 25% and 60% with varying degrees of current defoliation.

The current defoliation classes follow closely those used in operational sketch-mapping (Dorais and Kettela 1982). The percentage of current defoliation was estimated from the proportion of trees and proportion of the visible portion of the tree crowns with a red coloration and the intensity of that red coloration.

Defoliation levels and species composition of homogeneous sample areas were determined from interpretation of the vertical and oblique aerial photographs. Sample areas of the five defoliation classes, including the classification training areas, were genrally pure high density fir-spruce to spruce-fir. The classification training area for moderate cumulative defoliation was representative of the cumulative defoliation in the study area, which was often associated with varying levels of current defoliation within the same stand or on the same tree.

Analysis of classification capabilities was restricted to a case of five defoliation classes (severe, moderate, and light current defoliation, moderate cumulative defoliation, and healthy) in pure dense fir-spruce to spruce-fir stands.

Feature Selection

The nine bands of airborne MSS data were examined to determine their capability to separate levels of current defoliation from each other, from healthy conifers, and from cumulative defoliation. Ratio and differences of the bands were also investigated, as were principal components derived

TABLE 2. Features derived from the nine bands of the Multispectral Scanner.

Ratio of bands[1]
4/3, 5/3
6/3, 6/4, 6/5
9/3, 9/4, 9/6
11/3, 11/4, 11/6, 11/9
11/(3 + 4 + 5 + 6), 9/(3 + 4 + 5 + 6), 7/(4 + 5), 6/(4 + 5)
Difference between bands[2]
3-4
6-3, 6-4
9-3, 9-4, 9-6
11-4, 11-9
Principal components of all nine bands
1st, 2nd, and 3rd components of a specific sample area (equal areas of the five defoliation classes)
1st, 2nd, and 3rd components of a general sample area (entire study area)

[1] The ratio of two bands (A/B) is calculated by the equation: ratio = 128 × (intensity of band A ÷ intensity of band B).

[2] The difference of two bands (A-B) is calculated by the equation: difference = 128 − (intensity of band A − intensity of band B).

from the nine bands (Table 2). The capabilities of the features to separate defoliation classes were determined using Bhattacharyya distance (B-distance), a measure of statistical distance between classes (Kailath 1967). Class statistics of the defoliation classes were derived from sample areas representative of the defoliation classes. These sample areas were also used as training areas for supervised maximum likelihood classifications (classification training areas). The best single feature was selected as the feature with the largest average B-distance between classes. The best combination of two features was defined as the best single feature plus the feature in combination with the best single feature that produced the largest average B-distance between classes. The procedure was continued in a stepwise manner to determine useful combinations of two through *n* features.[1]

The feature selection procedure was used to determine features and feature combinations useful for differentiating defoliation levels for three cases:

1. current defoliation only [i.e., discriminating the four current defoliation classes (healthy, light, moderate, and severe) from each other]: the average of B-distances between these classes was used to determine useful features; results are appropriate for areas in which cumulative defoliation does not occur, or is minor;
2. mixed current and cumulative defoliation (i.e., discriminating the four current defoliation classes from one another and discriminating cumulative defoliation from current defoliation): the average B-distance between current defoliation classes, and between the moderate cumulative defoliation class and each of the current defoliation classes was used to determine useful features; results are

[1] In the forward selection procedure used, the features selected at each stage of *n* features depends on those previously selected. There is no provision for eliminating previously selected features. The best set of feature combinations at any stage derived by this analysis procedure therefore may not necessarily be the best overall combination of features if all possible combinations of *n* features were considered.

appropriate for differentiating defoliation conditions in an area with stands of current defoliation and stands of moderate cumulative defoliation;

3. cumulative versus current defoliation (i.e. discriminating cumulative defoliation from current defoliation): the average B-distance between the moderate cumulative defoliation class and each of the current defoliation classes was used in this case; this procedure will indicate whether any features are particularly beneficial for separating cumulative from current defoliation.

Classification Procedures

Supervised maximum likelihood techniques (Colwell 1983) were used to classify five defoliation classes: severe, moderate, and light current defoliation, moderate cumulative defoliation, and healthy. The classes were identified in dense forest stands with compositions ranging from pure fir-spruce to spruce-fir. The healthy class, however, was predominantly spruce-fir or spruce. Two additional healthy conifer classes, eastern cedar lowlands and tamarack, were included. The eastern cedar lowlands commonly occurred along stream courses and consisted predominantly of eastern white cedar with some other softwood species, including defoliated spruce and balsam fir. Several classes of mixed-wood were also included: softwood-hardwood (predominantly softwood), mixed-wood (approximately equal softwood and hardwood), and hardwood-softwood (predominantly hardwood). The softwoods of these mixed-wood classes were spruce and/or fir with current defoliation generally at the moderate level, often with some cumulative defoliation. The eastern cedar lowland, tamarack, and mixed-wood classes were used to test confusion with the five defoliation classes. They were also included to reduce commission errors due to: (1) areas of these classes being erroneously classified as one of the five defoliation classes, or (2) inclusions of defoliation within these classes being classified as the wrong defoliation class.

Classifications of the five defoliation classes, two additional healthy conifer classes, and three mixed-wood classes were completed using the best combinations of 2, 3, 4, 5, 7, and 9 bands and features as determined by the average B-distance between the five defoliation classes (Tables 3 and 4). Accuracies were determined by comparing the maximum likelihood classification of each pixel within a test sample area with the class of the sample area. The test sample areas were independent of the classification training areas.

RESULTS

Feature Selection

Spectral Bands

The best single bands, and useful sequence of bands in combination with one another, for discriminating among current defoliation classes are listed in Table 3. The near infrared bands (9, 8, and 10) were best for discriminating current defoliation, followed by the green bands (4 and 5). The red (6 and 7) and mid-infrared (11) bands were less useful. Results were similar if only the classes with current defoliation (severe, moderate, and light) are analyzed (Table 3). The combination of three bands included a near-infrared, red, and green band. There was little difference in the B-distance of the combination of four bands when the blue band (3) or mid-infrared band (11) was included as the fourth band. The three near-infrared bands were highly correlated with each other, and there was little value in including

TABLE 3. Bhattacharyya distance of single bands listed in order of decreasing B-distance, and B-distance of band combinations with bands listed in order of their entry into the sequence of band combinations.

1. Current defoliation only

(a) Single bands[1] (severe, moderate, light, healthy)

Band	9	8	10	4	5	7	6	11	3
B-distance	0.76	0.76	0.63	0.47	0.34	0.25	0.11	0.11	0.09

(b) Single bands[1] (severe, moderate, light)

Band	9	8	10	4	11	6	7	5	3
B-distance	0.46	0.43	0.38	0.12	0.10	0.07	0.05	0.05	0.03

(c) Combination of bands[2] (severe, moderate, light, healthy)

Band	9	6	4	3	11	5	10	7	8
B-distance	0.76	1.54	1.98	2.09	2.21	2.30	2.39	2.47	2.58

(d) Combination of bands[2] (severe, moderate, light)

Band	9	6	3	11	4	10	8	7	5
B-distance	0.46	1.16	1.35	1.48	1.58	1.67	1.73	1.86	1.93

2. Mixed current and cumulative defoliation (severe, moderate and light defoliation, moderate cumulative defoliation, healthy)

(a) Single bands[1]

Band	9	8	10	4	11	5	7	6	3
B-distance	0.63	0.63	0.53	0.41	0.32	0.29	0.21	0.20	0.17

(b) Combination of bands[2]

Band	9	6	4	11	5	3	8	7	10
B-distance	0.63	1.54	1.94	2.20	2.33	2.44	2.54	2.63	2.71

3. Cumulative versus current defoliation (moderate cumulative versus healthy and severe, moderate, and light current defoliation)

(a) Single bands[1]

Band	11	9	8	10	6	4	3	5	7
B-distance	0.65	0.44	0.43	0.38	0.33	0.31	0.29	0.23	0.15

(b) Combination of bands[2]

Band	11	9	6	4	5	3	8	7	10
B-distance	0.65	1.15	2.00	2.36	2.54	2.63	2.75	2.84	2.90

[1] Bhattacharyya distance for each band individually. The B-distance given is the average B-distance between the defoliation classes indicated in parentheses.

[2] Combination of best one through nine bands in order of entry into best sequence of bands. Bhattacharyya distance is that for the combined one through nine bands and is calculated as the average B-distance between the defoliation classes indicated in parentheses.

more than one near-infrared band. Band 7 gave poor separation of defoliation classes due to large variances in the reflectance within sample areas.

The band combinations for the case of mixed current and cumulative defoliation were similar to those for the case of current defoliation alone (Table 3). The cumulative versus current defoliation case in Table 3 gives the best

TABLE 4. Bhattacharyya distance of single features listed in order of decreasing B-distance, and B-distance of feature combinations with features listed in order of their entry into the sequence of feature combinations.

1. Current defoliation only

(a) Single features[1] (severe, moderate, light, healthy)

Feature	9/6	6/4	11/9	9	4/3	4	5	11/4	6	11	3
B-distance	1.24	0.90	0.78	0.76	0.59	0.47	0.34	0.12	0.11	0.11	0.09

(b) Single features[1] (severe, moderate, light)

Feature	9/6	11/9	6/4	9	11/4	4/3	4	11	6	5	3
B-distance	0.87	0.76	0.65	0.46	0.15	0.14	0.12	0.10	0.07	0.05	0.03

(c) Combination of features[2] (severe, moderate, light, healthy)

Feature	9/6	6/4	5	9	6	11/9	11	3	11/4	4	4/3
B-distance	1.24	1.85	2.11	2.25	2.50	2.66	3.07	3.16	3.24	3.29	3.35

(d) Combination of features[2] (severe, moderate, light)

Feature	9/6	6/4	11/9	11/4	9	6	3	11	4	4/3	5
B-distance	0.87	1.27	1.43	1.79	1.90	2.13	2.26	2.37	2.42	2.47	2.52

2. Mixed current and cumulative defoliation (severe, moderate and light current defoliation, moderate cumulative defoliation, healthy)

(a) Single features[1]

Feature	9/6	11/9	6/4	9	4/3	4	11/4	11	5	6	3
B-distance	1.09	0.95	0.94	0.63	0.47	0.41	0.36	0.32	0.29	0.20	0.17

(b) Combination of features[2]

Feature	9/6	6/4	11	11/9	9	6	5	3	11/4	4	4/3
B-distance	1.09	1.74	2.11	2.33	2.72	3.04	3.20	3.30	3.37	3.43	3.51

3. Cumulative versus current defoliation (moderate cumulative versus healthy and severe, moderate and light current defoliation)

(a) Single features[1]

Feature	11/9	6/4	9/6	11/4	11	9	6	4	3	4/3	5
B-distance	1.20	1.01	0.87	0.71	0.65	0.44	0.33	0.31	0.29	0.29	0.23

(b) Combination of features[2]

Feature	11/9	6/4	4	5	3	9/6	11	9	6	4/3	11/4
B-distance	1.20	1.93	2.35	2.55	2.64	2.76	3.21	3.46	3.56	3.67	3.76

[1] Bhattacharyya distance for each feature individually. The B-distance given is the average B-distance between the defoliation classes indicated in parentheses.

[2] Combination of best one through eleven features in order of entry into best sequence of features. Bhattacharyya distance is that for the combined one through eleven features and is calculated as the average B-distance between the defoliation classes indicated in parentheses.

single band and a useful sequence of bands in combination with each other for separating moderate cumulative defoliation from healthy and current defoliation. A feature selection test for differentiating severe cumulative defoliation from current defoliation and healthy stands was also conducted by calculating the average B-distance between these classes and a class of severe cumulative defoliation represented by a sample area of 100% mortality.

Important bands in combination with each other were, in order of importance: blue (3), a near-infrared (9), and mid-infrared (11). Leckie (1987) reports that it is advantageous to use blue, mid-infrared, and near-infrared bands to reduce confusion between current and cumulative defoliation when classifying current defoliation levels in areas where cumulative defoliation is present.

Features Derived from the Nine Spectral Bands

Use of features derived from the nine bands may improve classification capabilities and/or reduce the number of features required to provide accurate classifications. Thirty features were tested (Table 2), representing ratios and differences of bands within the main spectral regions (blue, green, red, near-infrared, and middle-infrared) and principal components derived from all nine bands. In cases where there were several highly correlated bands in the same spectral region, one band (generally the band with the best discrimination capability) was often used to represent that spectral region. For example, band 9 was used to represent the near-infrared region. Alternately, combinations of bands were also used to represent certain spectral regions, for example, 4 and 5 for the green. Some of these features were closely related. Related features were determined as those with high linear correlation coefficients, and by features whose importance was reduced when one of several related features was included in the sequence of best features.

Examination of the ratio features indicated several groupings of related features:

1. ratios involving the near-infrared band (9) and bands in the visible part of the spectrum [9/3, 9/4, 9/6, and 9/(3 + 4 + 5 + 6)]
2. ratios involving the mid-infrared band (11) and the visible bands [11/3, 11/4, 11/6, and 11/(3 + 4 + 5 + 6)]
3. ratios involving the blue band (3) and the other visible bands (4/3, 5/3, and 6/3), and
4. ratios involving the red versus green bands [6/5, 6/4, and 6/(4 + 5)].

The ratio of mid-infrared to near-infrared (11/9) was not closely related to other ratio features. The ratio of band 7 to the green bands [7/(4 + 5)] had low B-distances, indicating it was very poor for separation of defoliation classes. The best ratio features (for discriminating current defoliation levels) from each group of related features was determined from analyses of B-distances. They were, in order of importance, band ratios 9/6, 6/4, 11/9, 4/3, and 11/4. These band ratios were also important for the case of mixed current and cumulative defoliation. The single feature B-distance of the differences between two bands and the ratio of the same two bands were similar. The difference between bands 6 and 4, however, was the single most important feature for differentiating current defoliation classes of all the features tested.

Principal component techniques applied to Landsat MSS and airborne MSS data have been useful for forestry, especially for use in image enhancements (e.g., Kourtz and Scott 1978, Leckie and Dombrowski 1984). The first three principal components of all nine bands were determined for two cases: (1) a specific sample area comprised of approximately equal area of healthy stands, severe, moderate, and light current defoliation, and moderate cumulative defoliation; and (2) the entire study area. Analysis of enhancements produced from components of the two cases was unsuccessful at highlighting different defoliation levels as distinct, easily visually interpreted classes. Analysis of components for their capability to separate defo-

liation classes indicated that the first component for case 1 was highly correlated with the first component for case 2. The two second components were also highly correlated. The components for the specific sample area had slightly greater value in separating defoliation levels. On a single feature basis the first components were more important than the other components, but were not as important as several of the difference features, ratio features, or single bands. For example, the single feature B-distances for the first, second, and third component of the specific sample area were: 0.65, 0.25, and 0.02, respectively, for the current defoliation classes only; and 0.53, 0.47, and 0.08, respectively, for the case of mixed current and cumulative defoliation.

It is reasonable to assume that the best classification of defoliation classes might occur with a combination of ratio features that were among the best features derived from the nine spectral bands and the best individual spectral bands. Useful combinations of the nine spectral bands and features derived from these bands were, therefore, estimated by testing five ratio features (the best feature from each of the five groups of correlated features) and six spectral bands (bands 10 and 8 were not included as they were closely correlated to band 9, and band 7 was excluded because of its low capabilities for differentiating defoliation levels). The B-distances for the 11 final bands and features tested and sequence of features in combination with each other are given in Table 4. The ratios of the near-infrared to red band (9/6) and red to green band (6/4) were important. The importance of band ratio 9/6 is largely because of the change in near-infrared reflectance with defoliation. The high value of using band ratio 6/4 indicates the importance of the increase in red reflectance relative to green reflectance. For the case of cumulative versus current defoliation, band ratios 11/9 and 6/4 were important. However, this is largely due to their ability to separate moderate cumulative defoliation from healthy and light current defoliation classes. Band 11 or the ratio of bands 11/6 and 11/4 showed better separation of the cumulative defoliation class from the moderate and severe current defoliation classes.

Classification Results

Tables 5 and 6 give classification accuracies of the five defoliation classes for classifications using all nine bands and the best combination of four bands as estimated by the stepwide B-distance analysis procedure for separating the five defoliation classes (Table 3). The accuracies of the best combinations of four through nine features (bands and derived features) obtained by the B-distance analysis indicated similar results. There was considerable confusion between adjacent defoliation classes in the sequence of current defoliation (i.e., severe, moderate, light, and healthy). Confusion between the severe and moderate current defoliation was particularly high. This suggests that perhaps only three current defoliation classes, heavy (a combination of severe and moderate classes), light, and healthy, can be reliably classified. Classification accuracy for the heavy class was approximately 75%. Average accuracy for four defoliation classes (heavy, light, healthy, and moderate cumulative defoliation) was approximately 65% to 69%, 4% to 6% higher than for the five defoliation classes.

There was also confusion between the severe and moderate (or heavy) current defoliation classes and the moderate cumulative defoliation class. The confusion with current defoliation differs under different conditions of cumulative defoliation (e.g., more severe or less severe). In areas where no

TABLE 5. Classification accuracy (%) for classification of ten classes using nine bands.

	Maximum likelihood class								
	Cumulative	Severe	Moderate	Light	Healthy	Others[1]	Unclassified	Accuracy	Misclassification
Cumulative	63.3	5.3	11.4	2.6	0.2	5.9	11.3	63.3	28.7
Severe	6.9	68.7	18.0	2.9	0.2	1.0	2.3	68.7	29.7
Moderate	7.2	14.7	49.8	8.9	0.6	11.0	7.8	49.8	46.0
Light	0.8	3.3	14.2	71.4	4.2	5.0	1.1	71.4	27.6
Healthy	0.3	0.2	3.9	4.4	65.4	15.9	9.9	65.4	27.4

[1] Eastern cedar lowlands, tamarack, softwood-hardwood, mixed-wood, hardwood-softwood.

TABLE 6. Classification accuracy (%) for classification of ten classes using the best combination of four bands for separating the five defoliation classes (i.e., bands 9, 6, 4, and 11).

	Maximum likelihood class								
	Cumulative	Severe	Moderate	Light	Healthy	Others[1]	Unclassified	Accuracy	Misclassification
Cumulative	63.9	10.4	9.0	0.9	0.2	5.7	9.9	63.9	29.0
Severe	8.2	65.1	18.9	3.7	0.2	2.3	1.6	65.1	33.9
Moderate	8.0	15.6	50.2	8.0	1.3	14.0	2.9	50.2	48.3
Light	0.4	5.5	8.5	74.6	4.1	6.1	0.8	74.6	24.7
Healthy	0.6	0.2	3.3	13.0	55.9	20.5	6.5	55.9	41.4

[1] Eastern cedar lowlands, tamarack, softwood-hardwood, mixed-wood, hardwood-softwood.

cumulative defoliation is present, the classification accuracy of heavy current defoliation is expected to be high. Accuracy was estimated to be approximately 80% and average accuracy for the heavy, light, and healthy classes was estimated to be 70% to 73%.[2] In an operational survey, only two defoliation classes (heavy and light current defoliation) plus identification of a single class of healthy conifers, regardless of species composition, may be required (i.e., accurate identification of the type of healthy conifer is not required). For a case of no cumulative defoliation, and a healthy conifer class including the healthy mixed fir and spruce, tamarack, and cedar lowlands classes, accuracy was estimated to be 75% to 80%.

There was some confusion of defoliated areas with the other forest classes (Tables 5 and 6). A more serious problem is areas of other forest types being classified as one of the defoliation classes. For example, approximately 25% of eastern cedar lowland sample areas and 25% to 30% of softwood-hardwood sample areas were classified as one of the defoliation classes. Although there was defoliation of some of the fir and spruce associated with these forest types, a reliable classification of the correct defoliation level was not possible.

Figure 1 gives the classification accuracy for four defoliation classes (heavy and light current defoliation, moderate cumulative defoliation, and healthy) plotted against number of bands or features in the sequence of bands and feature combinations of Tables 3 and 4 (mixed current and cumulative defoliation case). There was little advantage using the combinations of features instead of the combinations of bands; classification accuracies were similar (Figure 1). A classification of four bands or features was sufficient. Total area estimates for each of the defoliation classes were generally stable for classifications using four or more bands or features. There was, however, a decrease in the number of pixels classified as one of the five defoliation classes as the number of features increased. This was due to an increase in the number of unclassified pixels. Commission errors became important if only two or three bands or features were used; for example, some areas of floating log debris and some shoreline boundaries were classified as defoliation.

SUMMARY AND DISCUSSION

The best single bands for separating levels of current defoliation were the near-infrared (8, 9, and 10), followed by green (4 and 5). The red band (6) and mid-infrared band (11) were of lesser importance. There was a decrease in near-infrared and green band reflectance with increasing current defoliation, but the difference in reflectance between severe, moderate, and light current defoliation was small for the other visible bands and the mid-infrared band (Leckie 1987). The ratios of a near-infrared channel with a visible or combination of visible channels, especially the ratio of bands 9 and 6 (9/6), and the difference or ratio of the red and green band (6–4 and 6/4) were important single features for separating current defoliation classes. The best combination of four bands as determined by the stepwise B-distance analysis was 9, 6, 4, and 3. Similarly, the best combination of four ratio features and bands was the ratio of bands 9 and 6 (9/6), the ratio of bands 6 and 4 (6/4), and bands 5 and 9.

[2] Estimated by eliminating all pixels classified as cumulative defoliation from the analysis of accuracy.

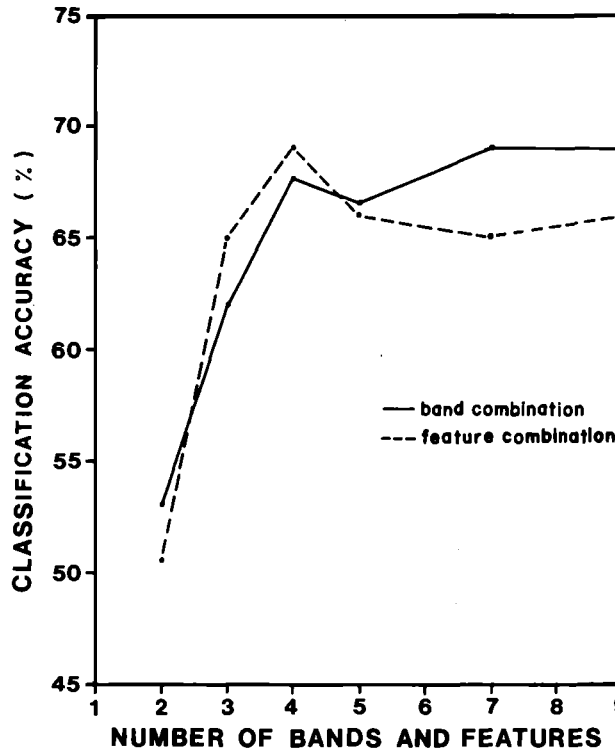

FIGURE 1. Mean classification accuracy for four defoliation classes (heavy and light current defoliation, moderate cumulative defoliation, and healthy) for classifications using the best combinations of 2, 3, 4, 5, 7, and 9 bands and features (Table 3 and 4, mixed current and cumulative defoliation case).

B-distance analysis indicated that the mid-infrared band (11) was best for separating moderate cumulative defoliation from current defoliation. Overlap of the airborne MSS band intensities of areas of moderate cumulative defoliation with those of current defoliation was least in band 11 (Leckie 1987). The best band combination for classifying the four current defoliation levels and moderate cumulative defoliation (using the stepwise B-distance analysis procedure) was bands 9, 6, 4, and 11; the best feature combination was the ratio of band 9 and 6 (9/6), the ratio of band 6 and 4 (6/4), band 11, and the ratio of band 11 and 9 (11/9). There was little difference in classification accuracy when using the best band or best feature combinations.

Three levels of current defoliation (heavy, light, and healthy) in dense fir-spruce to spruce-fir stands can be classified. In some cases it may be possible to classify four levels of current defoliation. Classification accuracy for three current defoliation classes (heavy, light, and healthy) was approximately 67% for a case where moderate cumulative defoliation was present. Most confusion is between adjacent classes or between heavy current defoliation and moderate cumulative defoliation. Current and cumulative defoliation may be confused, except perhaps when cumulative defoliation is severe. Errors can be minimized by using a mid-infrared band (11) and, possibly, a blue band (3) if cumulative defoliation is severe. In cases where cumulative defoliation does not occur, accuracies for classifying current defoliation classes are approximately 70% to 73%. If only light and heavy de-

foliation areas are required (i.e., classification of healthy conifer classes not required), classification accuracy can be expected to be 75% to 80%.

The classifications obtained for the airborne MSS data were moderately successful. Other limitations of classification of airborne MSS data exist. Results of this study are relevant to classification capabilities in dense pure fir-spruce and spruce-fir stands. Classification of defoliation in mixed-wood stands is difficult (Leckie 1987). Varying proportions of hardwoods and softwoods within the area covered by each pixel cause confusion in the classification of defoliation levels. Similar difficulties occur with open stands (Leckie and Gougeon 1981). In addition, radiometric distortions across an image due to sun-object-viewer geometry are often different for softwoods versus hardwoods. It was not possible to classify the data of this study for defoliation in mixed-woods due to the differing radiometric distortions for softwoods versus hardwoods. Fir and spruce have different spectral reflectances. The proportion of fir versus spruce in a stand does cause some confusion in classification, especially for the extreme case of pure fir and spruce stands (Leckie 1987). There was also some confusion of defoliation classes with other forest types.

Good classifications of cumulative defoliation in dense fir-spruce forests are possible (Leckie and Gougeon 1981), and this study indicates moderate capabilities for classifying current defoliation. Although classification techniques are useful under certain circumstances, they will become suitable for widespread operational use only after problems associated with the analysis of data have been resolved.

There are several possibilities for resolving these problems and improving the capabilities of airborne scanner data for defoliation classification. The classification capabilities of current defoliation may be improved by the use of optimized wavelength bands. A study to define these wavelength bands for both current and cumulative defoliation has been initiated, with preliminary results showing opportunities for better defoliation assessment using optimized wavelength bands (Teillet et al. 1985). An optimization in the red region of the spectrum may be particularly useful. Leckie (1987) reports that there is little difference in recorded intensities of airborne MSS data in the red bands of the Daedalus model 1260 scanner (bands 6 and 7 of Table 1) with current defoliation level. Ahern et al. (1986), through analysis of color composites and enhancements of airborne MSS (Daedalus model 1260) data and MEIS II (Multispectral Electro-Optical Imaging Scanner II) imagery, showed that current defoliation could be detected on MEIS II data while it could not on the Daedalus 1260 data. The better capability of the MEIS II scanner was traced to the better separation of defoliation by the red band used with the MEIS II (0.60–0.69 μm), as compared with those of the Daedalus scanner (band 7: 0.63–0.70 μm, or band 6: 0.59–0.65 μm).

A possible solution to the problem of confusion due to varying species proportion or varying stand densities of each pixel is the use of change detection techniques in which images from different times of the year, or from successive years, are digitally overlain and compared. Since stand density and species composition can generally be assumed to be constant over time for each pixel, variations among the changes in intensity of pixels can be related more closely to defoliation. Overlay of imagery with existing forest inventory information on a Geographic Information System would provide auxiliary information regarding species composition, density, and age which, if accurate, could aid in classifying defoliation. An advantage may be gained by tilting the scanner forward or aft so that it is viewing the forest at

an oblique angle. The field of view of the scanner will generally be dominated by the upper parts of the forest canopy, thus reducing the effects of differing crown closure and ground cover. In addition, the upper portions of the tree often appear more severely discolored due to budworm attacks, possibly accentuating apparent defoliation when viewed obliquely. Techniques need to be developed and tested. The problem of radiometric distortion across the images due to sun-object-viewer geometry also needs further investigation.

Recent advancements in airborne multispectral scanners facilitate developments needed to improve techniques for spruce budworm defoliation assessment. For example, the MEIS II airborne scanner is a linear array detector sensor system with eight spectral bands, the wavelength of which can be selected by use of spectral filters (McColl et al. 1984). Filters with optimized wavelength bands for spruce budworm defoliation assessment can be utilized. Enhancements of MEIS II data have been shown to be useful for softwood species discrimination (Leckie and Dombrowski 1984), and Ahern et al. (1986) indicated the potential for visual intepretation of MEIS II data for current spruce budworm defoliation assessment. Another key development is the use of inertial navigation system data to efficiently and accurately correct airborne multispectral scanner data geometrically (Gibson 1984). It is, therefore, possible to directly relate airborne data (such as MEIS II imagery) and subsequent interpretations and classifications of the data to cartographic base maps (e.g., forest inventory maps), especially those on a Geographic Information System. Also, images from different times can be registered to facilitate change detection techniques.

Results of this study and others suggest that the advantages of airborne MSS data, along with new developments in airborne sensors and systems, may provide more detailed and accurate information on spruce budworm defoliation. This will meet a growing demand.

LITERATURE CITED

AHERN, F. A., W. J. BENNETT, and E. G. KETTELA. 1986. An initial evaluation of two airborne imagers for surveying spruce budworm defoliation. Photogramm. Eng. & Remote Sensing. 52:1647–1654.

ARCHAMBAULT, L. 1983. Impact of defoliation caused by the spruce budworm on volume growth in three fir stands. Can. For. Serv. Res. Notes 3:17–19.

ASHLEY, M. D., J. REA, and L. WRIGHT. 1976. Spruce budworm damage evaluations using aerial photography. Photogramm. Eng. & Remote Sensing 42:1265–1272.

BATZER, J. 1973. Net effect of spruce budworm defoliation on mortality and growth of balsam fir. J. For. 71:34–37.

CIESLA, W. M. 1974. Forest insect damage from high altitude color IR photos. Photogramm. Eng. & Remote Sensing 40:683–689.

COLWELL, R. N. (ed.). 1983. Manual of remote sensing. Ed. 2. Am. Soc. Photogramm. Falls Church, VA. P. 1045–1051.

DORAIS, L., and E. G. KETTELA. 1982. A review of entomological survey and assessment techniques used in regional spruce budworm, *Choristoneura fumiferana* (Clem.) surveys and in assessment of operational spray programs. Rep. Comm. Standardization of Survey and Assessment Techniques. Eastern Spruce Budworm Counc. Ministère de l'Énergie et des Ressources, Québec. 43 p.

GIBSON, J. R. 1984. Processing stereo imagery from line imagers. P. 471–487 *in* Proc. 9th Can. Symp. Remote Sensing, St. John's, Nfld.

HARRIS, J. W. E., and A. F. DAWSON. 1979. Evaluation of aerial forest pest damage survey techniques in British Columbia. Can. For. Serv., Pac. For. Cent. Inf. Rep. BC-X-198. 22 p.

HARRIS, J. W. E., A. F. DAWSON, and D. GOODENOUGH. 1978. Evaluation of Landsat data for

forest pest detection and damage appraisal surveys in British Columbia. Can. For. Serv. Pac. For. Cent. Inf. Rep. BC-X-182. 12 p.

KAILATH, T. 1967. The divergence and Bhattacharyya distance measures in signal selection. IEEE Trans. Comm. Tech. 15:52–60.

KETTELA, E. G. 1983. A cartographic history of spruce budworm defoliation from 1967 to 1981 in eastern North America. Can. For. Serv. Inf. Rep. DPC-X-14. 8 p.

KLEINSCHMIDT, S. M., G. L. BASKERVILLE, and D. S. SOLOMON. 1980. Reduction of volume increment in fir/spruce stands due to defoliation by spruce budworm. Univ. New Brunswick, Faculty of For., Frederiction. 37 p.

KOURTZ, P. H., and A. J. SCOTT. 1978. An improved enhancement technique and its application to forest fire management. P. 72–78 *in* Proc. 5th Can. Symp. Remote Sensing. Victoria, B.C.

LECKIE, D. G. 1987. Factors affecting defoliation assessment using airborne multispectral scanner data. Photogramm. Eng. & Remote Sensing. 53:1665–1674.

LECKIE, D. G., and A. DOMBROWSKI. 1984. Enhancement of high resolution MEIS II data for softwood species discrimination. P. 617–626 *in* Proc. 9th Can. Symp. Remote Sensing. St. John's, Nfld.

LECKIE, D. G., and F. A. GOUGEON. 1981. Assessment of spruce budworm defoliation using digital airborne MSS data. P. 190–196 *in* Proc. 7th Can. Symp. Remote Sensing. Winnipeg, Man.

MACLEAN, D. A. 1980. Vulnerability of fir/spruce stands during uncontrolled spruce budworm outbreaks: A review and discussion. For. Chron. 56:213–221.

MADDING, R. P., and H. E. HOGAN. 1978. Detection and mapping of spruce budworm defoliation in northern Wisconsin using digital analysis of Landsat data. P. 285–300 *In* Proc. 44th Annu. Meet. Am. Soc. Photogramm. Washington, D.C.

MCCOLL, W. D., R. A. NEVILLE, and S. M. TILL. 1984. Multi-detector Electro-optical Imagery Scanner (MEIS II). P. 71–77 *in* Proc. 8th Can. Symp. Remote Sensing. Montreal, Québec.

MILLER, C. A. 1977. Feeding impact of spruce budworm on balsam fir. Can. J. For. Res. 7:76–84.

MURTHA, P. A. 1973. Spruce Budworm Damage in Fundy National Park, New Brunswick. Natl. Park For. Serv. Rep. #6. For. Manage. Inst., Can. For. Serv. Ottawa, Ont. 12 p.

PIENE, H. 1980. Effects of insect defoliation on growth and foliar nutrients of young balsam fir. For. Sci. 26:665–673.

TEILLET, P. M., et al. 1985. Spectral measurements of tree defoliation. P. 511–516 *in* Proc. 3rd Int. Colloq. Spectral Signatures of Objects in Remote Sensing, Les Arcs, France.

ZWICK, H. H., W. D. MCCOLL, and H. R. EDEL. 1980. The CCRS DS1260 Airborne Multispectral Scanner (MSS). P. 643–648 *in* Proc. 9th Can. Symp. Remote Sensing. Halifax, N.S.